

ADVANCED TECHNOLOGY RADAR RESEARCH CENTER

By

H. S. Mayne and R. F. Broderick**

TR-68-10

NAS 9-9828

Wave Propagation Laboratories
Department of Electrical Engineering

N71-14755

(ACCESSION NUMBER)

FACILITY FORM 602

19
(PAGES)

CR-114803
(NASA CR OR TMX OR AD NUMBER)

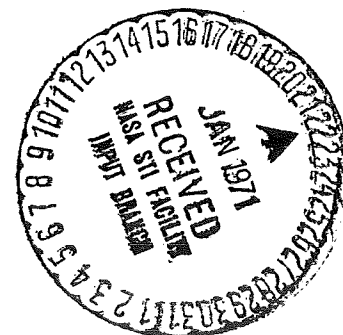
(THRU)

GB

(CODE)

07

(CATEGORY)



UNIVERSITY OF HOUSTON
Cullen College of Engineering
3001 Cullen Boulevard
Houston, Texas 77004

This work is sponsored by NASA Manned Spacecraft Center, Houston, Texas, under Contract NAS 9-9828.

Also derive from NASA Manned Spacecraft Center, Houston, Texas.

Reproduced by
**NATIONAL TECHNICAL
INFORMATION SERVICE**
Springfield, Va. 22151

07

NOTICE TO USERS

Portions of this document have been judged by the Clearinghouse to be of poor reproduction quality and not fully legible. However, in an effort to make as much information as possible available to the public, the Clearinghouse sells this document with the understanding that if the user is not satisfied, the document may be returned for refund.

If you return this document, please include this notice together with the IBM order card (label) to:

Clearinghouse
Attn: 152.12
Springfield, Va. 22151

11-70-62

THE STATISTICS OF RADAR RETURN
FROM AN EXTENDED SURFACE

Abstract

Usually the mean square value or the radar scattering cross-section area of the radar return from a random rough surface is employed in general work. The altitude or range dependence is not included in the specification of such results. In the case of decreasing altitudes, the area beamwidth covered by the radar may approach the dimensions of the order of the surface decorrelation distance whereupon the local surface mean and variance have significant effect on the backscattered energy and its statistics. Simultaneous measurements from a scatterometer as well as a doppler radar system mounted in a helicopter are used to illustrate this significant change in the radar return statistics.

Introduction

For a random rough surface, the scattered power $\langle E_2 E_2^* \rangle$ may be expressed in terms of the surface heights ξ_1, ξ_2 as shown by Beckmann, et al. (1963) or

$$\langle E_2 E_2^* \rangle = \frac{E_0^2 F^2(\theta_1, \theta_2, \theta_3)}{A} \iint_{-X/2}^{X/2} \iint_{-Y/2}^{Y/2} \langle e^{i k_x (z_1 - z_2)} e^{i k_y (y_1 - y_2)} \rangle dx_1 dx_2 dy_1 dy_2 \quad (1)$$

where $\langle \rangle$ = statistical average.

$$\xi_1 = \xi(x_1, y_1) \quad , \quad \xi_2 = \xi(x_2, y_2)$$

$$E_N = \frac{i k e^{i k R_0} A}{2 \pi R_0}$$

$$A = 4 \pi Y$$

$$F = \frac{1 + \cos \theta_1 \cos \theta_2 - \sin \theta_1 \sin \theta_2 \cos \theta_3}{\cos \theta_1 + \cos \theta_2}$$

$$V_x = \frac{2\pi}{\lambda} (\sin \theta_1 - \sin \theta_2 \cos \theta_3)$$

$$V_y = -\frac{2\pi}{\lambda} (\sin \theta_1 \sin \theta_3)$$

$$V_z = -\frac{2\pi}{\lambda} (\cos \theta_1 + \cos \theta_2)$$

The ratio of the scattered power to incident power is typically expressed in terms of a reflection coefficient $\langle \rho \rho^* \rangle$ and considering a mean and variance

$$\langle |\rho|^2 \rangle = \langle \rho \rho^* \rangle = \langle \rho \rangle \langle \rho^* \rangle + D \{ \rho \} \quad (2)$$

The radar equation for an extended surface can be expressed in terms of the altitude (H) and depression angle (θ) as

$$\frac{S}{N} = \frac{P_t G \lambda^2 \cos \theta \sigma_b}{4\pi R^2 (k T (F) L \bar{N} F)} \quad (3)$$

where the backscattering coefficient $R(\theta)$ is related to the backscattering cross-section (σ^o) as

$$\sigma^o(\theta) = 4\pi R(\theta) \cos \theta \quad (4)$$

and also considered to be composed of a mean value $\langle R(\theta) \rangle$ and variance $D\{R(\theta)\}$

where S/N = signal to noise ratio

P_t = transmitted power

G = antenna gain

λ = transmitted wavelength

k = Boltzman's constant

$\bar{N}F$ = receiver noise figure

(F) = receiver bandwidth, and

L = system losses.

A reference to Figure 1 shows that the backscattering cross-section for beam incident at an angle (θ_i) on a surface with slope (ϕ) is

$$\sigma^o = 4\pi R(\theta) \cos(\theta_i - \phi) \quad (5)$$

where the smooth surface ($\phi = 0$) produces the usual expression of Eq. (4) and a random rough surface with non-zero ϕ and randomly distributed heights produces the expanded expression

$$\langle \sigma^o \rangle = 4\pi R(\theta) \{ \cos \theta_i \langle \cos \phi \rangle + \sin \theta_i \langle \sin \phi \rangle \} \quad (6)$$

Equations (4) and (5) indicate the existence of a smooth surface component plus two components due to the surface roughness or

$$\begin{pmatrix} \sigma_{\theta} \\ \sigma_{\parallel} \\ \sigma_{\perp} \end{pmatrix} = 4\pi R(\theta) \begin{pmatrix} \cos \theta_0 \\ \cos \theta_0 \langle \cos \phi \rangle \\ \sin \theta_0 \langle \sin \phi \rangle \end{pmatrix} \quad (7)$$

Expressing the backscattering coefficient $R(\theta)$ in exponential form with slope R_R and relating the mean absolute square of the reflection coefficient to the specular reflection coefficient for smooth earth, one obtains

$$\langle |R(\theta)|^2 \rangle = \langle |R^s|^2 \rangle R^2(\theta) e^{-2R_R |\theta|} \quad (8)$$

or

$$\frac{\langle |R(\theta)|^2 \rangle}{R^2(\theta) e^{-2R_R |\theta|}} = \langle |R^s|^2 \rangle + D \{ |R^s|^2 \} \quad (9)$$

and from Eq. (7) the variance $D \{ |R^s|^2 \}$ is considered to consist of both horizontal and vertical components, or

$$D \{ |R^s|^2 \} = \mu_{\parallel}^2 + \mu_{\perp}^2 \quad (10)$$

Normally Distributed Directional Slopes

The rough surface $\zeta(x, y)$ with directional slope angles ϕ_1, ϕ_2 in the corresponding x and y directions would be normally distributed directional slopes $\tan \phi_1, \tan \phi_2$ when the surface heights are normally distributed.

$$p(\tan \phi_1, \tan \phi_2) = \frac{1}{2\pi \phi_0^2 \sqrt{1-\rho^2}} \exp\left(-\frac{\tan^2 \phi_1 + \tan^2 \phi_2 - 2 \tan \phi_1 \tan \phi_2 \rho}{2\pi \phi_0^2 [1-\rho^2]}\right) \quad (11)$$

A calculation of the Jacobian relating the probability density functions of the slopes $(\tan \phi_1, \tan \phi_2)$ to that of the angles (ϕ_1, ϕ_2) gives:

$$J(\phi_1, \phi_2) = \left| \frac{\partial(\tan \phi_1, \tan \phi_2)}{\partial(\phi_1, \phi_2)} \right| = \tan \phi_1 \tan \phi_2 (1 - \tan \phi_1 \tan \phi_2 \rho) \quad (12)$$

Noting the series expansion of $\tan \phi$ and $\tan^2 \phi$ as given below

$$\tan \phi = \frac{\phi}{\pi} \sum_{k=1}^{\infty} \frac{1}{(2k-1)^2 - \left(\frac{\phi}{\pi}\right)^2} \quad (13)$$

$$\tan^2 \phi = \frac{\phi^2}{\pi^2} \sum_{k=1}^{\infty} \frac{(2k-1)^2 - \frac{2}{\pi^2} \phi^2}{\left[(2k-1)^2 - \left(\frac{\phi}{\pi}\right)^2\right]^2} \quad (14)$$

In the case of small angles $(\phi_1, \phi_2 \ll 1)$ $\tan \phi$ and $\tan^2 \phi$ may be approximated by ϕ and ϕ^2 respectively. The usual random variable transformation of the $p(\tan \phi_1, \tan \phi_2)$ into $p(\phi_1, \phi_2)$ yields:

$$p(\phi_1, \phi_2) = J(\phi_1, \phi_2) p(\tan \phi_1, \tan \phi_2) \quad (15)$$

which when approximated becomes

$$p(\phi_1, \phi_2) \approx \frac{1}{2\pi \phi_0^2 \sqrt{1 - \rho^2}} \exp - \left(\frac{\phi_1^2 + \phi_2^2 - 2\rho \phi_1 \phi_2 \cos \theta}{2\pi \phi_0^2 (1 - \rho^2)} \right) \quad (16)$$

where $J(\phi_1, \phi_2)$ is approximated as unity for $\phi_1, \phi_2 \ll 1$. Furthermore, for small angles $\phi_1, \phi_2 \ll 1$, one may obtain these expressions for the average of $\sin \phi$, $\cos \phi$:

$$\begin{pmatrix} \langle \sin \phi \rangle \\ \langle \cos \phi \rangle \end{pmatrix} = \int_{-\infty}^{\infty} \int_{-\infty}^{\infty} \begin{pmatrix} \sin \phi_1 \cos \phi_2 \\ \cos \phi_1 \cos \phi_2 \end{pmatrix} p(\phi_1, \phi_2) d\phi_1 d\phi_2 \quad (17)$$

which result in the following simplification:

$$\begin{pmatrix} \langle \sin \phi \rangle \\ \langle \cos \phi \rangle \end{pmatrix} = e^{-\frac{\phi_0^2}{2}} \begin{pmatrix} \cos H(\phi_0^2 \rho \cos \theta) \\ \cos H(\phi_0^2 \rho \sin \theta) \end{pmatrix} \quad (18)$$

At an altitude H and beamwidth \bar{B} , the distance along the velocity vector illuminated by the beamwidth is

$$d_1 = H \left\{ \tan \left(\theta_0 + \frac{\bar{B}}{2} \right) - \tan \left(\theta_0 - \frac{\bar{B}}{2} \right) \right\} \quad (19)$$

whereas a corresponding distance along the y-axis is

$$d_2 = 2 H \tan \frac{\bar{B}}{2} \quad (20)$$

Assuming independent correlation in the x and y directions and using an exponential form of the autocovariance function for ϕ

$$R_\phi(\xi, \eta) = \phi_0^2 \exp \left\{ -\xi/\xi_0 - \eta/\eta_0 \right\} \quad (21)$$

for a rectangular aperture, one obtains

$$\begin{pmatrix} A_u^2 \\ A_v^2 \end{pmatrix} = \frac{4e^{-k^2 d_1^2}}{d_1 d_2} \int_0^{d_1} \int_0^{d_2} (1 - \xi_1)(1 - \xi_2) \begin{pmatrix} \cos\{k d_1 (\xi_1^2 + \xi_2^2)\} \\ \sin\{k d_1 (\xi_1^2 + \xi_2^2)\} \end{pmatrix} d\xi_1 d\xi_2 \quad (22)$$

or the rough surface contributions are

$$A_u^2 = \frac{4e^{-k^2 d_1^2}}{d_1 d_2} \sum_{m=1}^{\infty} \frac{(d_1^2)^{m-1}}{(m-1)!} \left\{ \left(\frac{d_2}{2m d_1} \right) \left[1 - \frac{d_2}{2m d_1} \left(1 - e^{-\frac{2m d_1^2}{d_2}} \right) \right] \right\} \left\{ \left(\frac{d_1}{2m d_2} \right) \left[1 - \frac{d_1}{2m d_2} \left(1 - e^{-\frac{2m d_2^2}{d_1}} \right) \right] \right\} \quad (23)$$

$$A_v^2 = \frac{4e^{-k^2 d_1^2}}{d_1 d_2} \sum_{m=1}^{\infty} \frac{(d_1^2)^{m-1}}{(m-1)!} \left\{ \left(\frac{d_2}{2m d_1} \right) \left[1 - \frac{d_2}{2m d_1} \left(1 - e^{-\frac{2m d_1^2}{d_2}} \right) \right] \right\} \left\{ \left(\frac{d_1}{2m d_2} \right) \left[1 - \frac{d_1}{2m d_2} \left(1 - e^{-\frac{2m d_2^2}{d_1}} \right) \right] \right\} \quad (24)$$

where in the case of pulse-width limiting, the limits of integration (d_1, d_2) are changed correspondingly. The constant component and fluctuating or Rayleigh components may be expressed as a random vector sum comprised of the constant and Rayleigh vectors (Beckmann and Spizzichino, 1963)

$$R_0^2 = \frac{e^{-k^2 d_1^2}}{A_u^2 + A_v^2} \quad (25)$$

and unless $\xi_1 \gg d_1, \xi_2 \gg d_2$ the major contributions are from the rough surface effects.

Measurements

A series of low altitude tests (1,000 to 50 feet altitude) were run at White Sands, New Mexico to determine the surface variance effects without extreme beamwidth averaging. A typical radar cross-section curve (mean and standard deviation) processed from a 13.3 Gc scatterometer (Broderick, 1967) is shown in Figure 2. A time history of the cross-section is shown in Figure 3 with a typical probability density function of the radar cross-section shown in Figure 4. An illustration of the effects of beamwidth averaging is shown in Figure 5, where it can be seen that the variance is highest at the lowest altitude and similarly a smaller surface decorrelation distance (a distance at which the autocorrelation function decays to e^{-1} times its maximum value) can be observed at the lower altitudes. The particular site shown consisted of relatively flat desert area with surface heights (sand dunes) in the range of one to two feet.

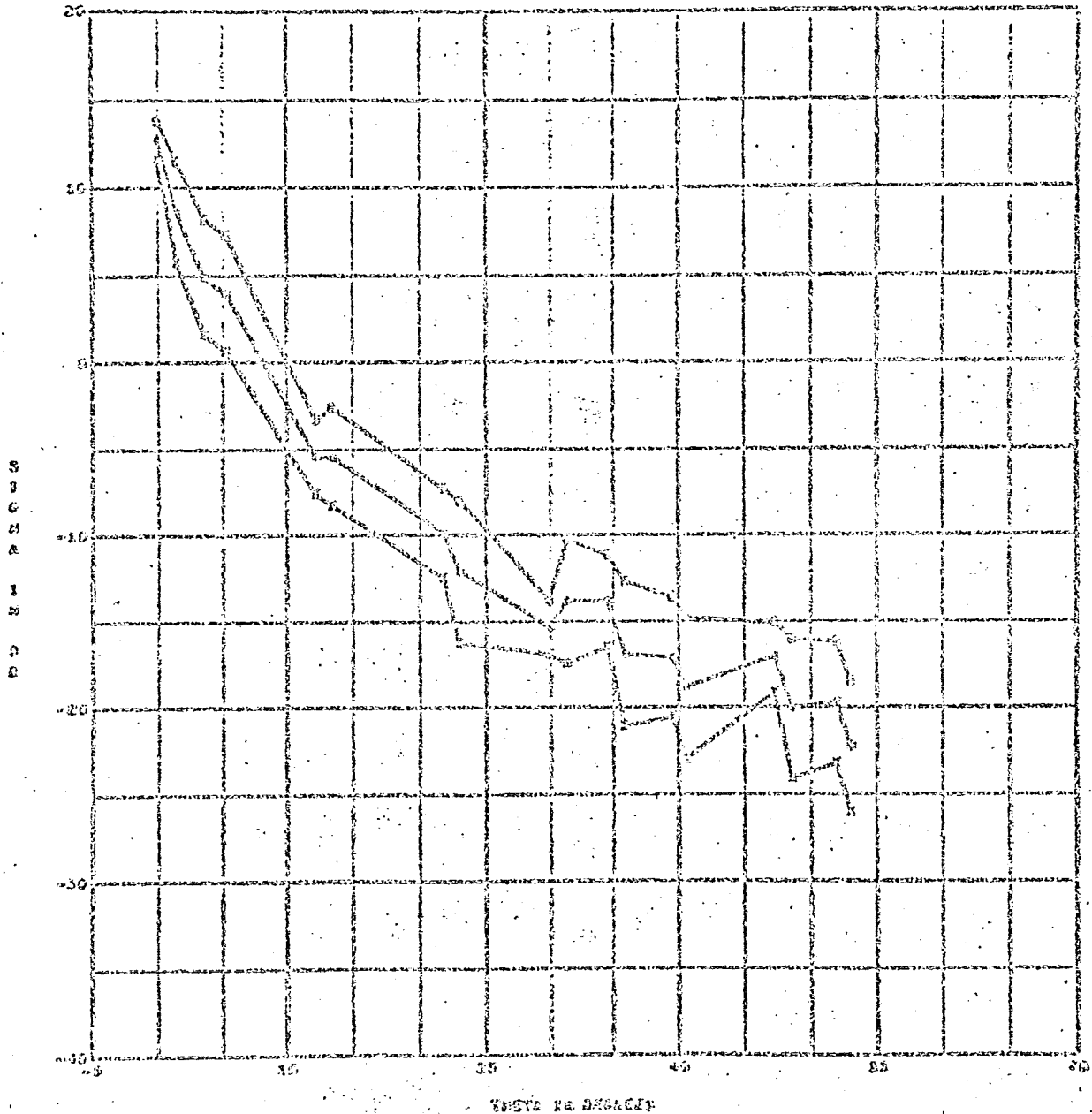
The doppler radar serves as another method of observing the effects of the surface variance. Again referring to Figure 1, the doppler expression for the beam incident angle (θ_0) and surface slope (ϕ) is

$$\omega_d = \frac{4\pi V}{\lambda} \sin(\theta_0 + \phi) \quad (26)$$

and for a random rough surface with ϕ non-zero and random distributed

$$\langle \omega_d \rangle = \frac{4\pi V}{\lambda} \left(\sin \theta_0 \langle \cos \phi \rangle + \cos \theta_0 \langle \sin \phi \rangle \right) \quad (27)$$

DATA FROM FLU & ZGOPY CURVE 3 W/ HAY WIND/ON/RE/10/07/67 2312



STARS 24 22 0.418
 STG 14 22 11.470
 A AVERAGE
 C AVERAGE - STD DEV
 E AVERAGE - STD DEV

PHYSICAL SCIENCE AND SPACE ADMINISTRATION
 WASHINGTON FIELD OFFICE CENTER - WASHINGTON
 ATTY GEN
 SCATTERING MISSION
 FLIGHT 0 LINE 0
 RUN 0 SIZE 2

FIGURE 2. RADAR CROSS-SECTION CURVES

SIGMA PLAYS NEAR FLY 2 LINE 3 RUN 3 SITE WSHH REQ 251 APT

SIGMA 1
SIGMA 2

4
2

SIGMA 3
SIGMA 4

0

SIGMA 5

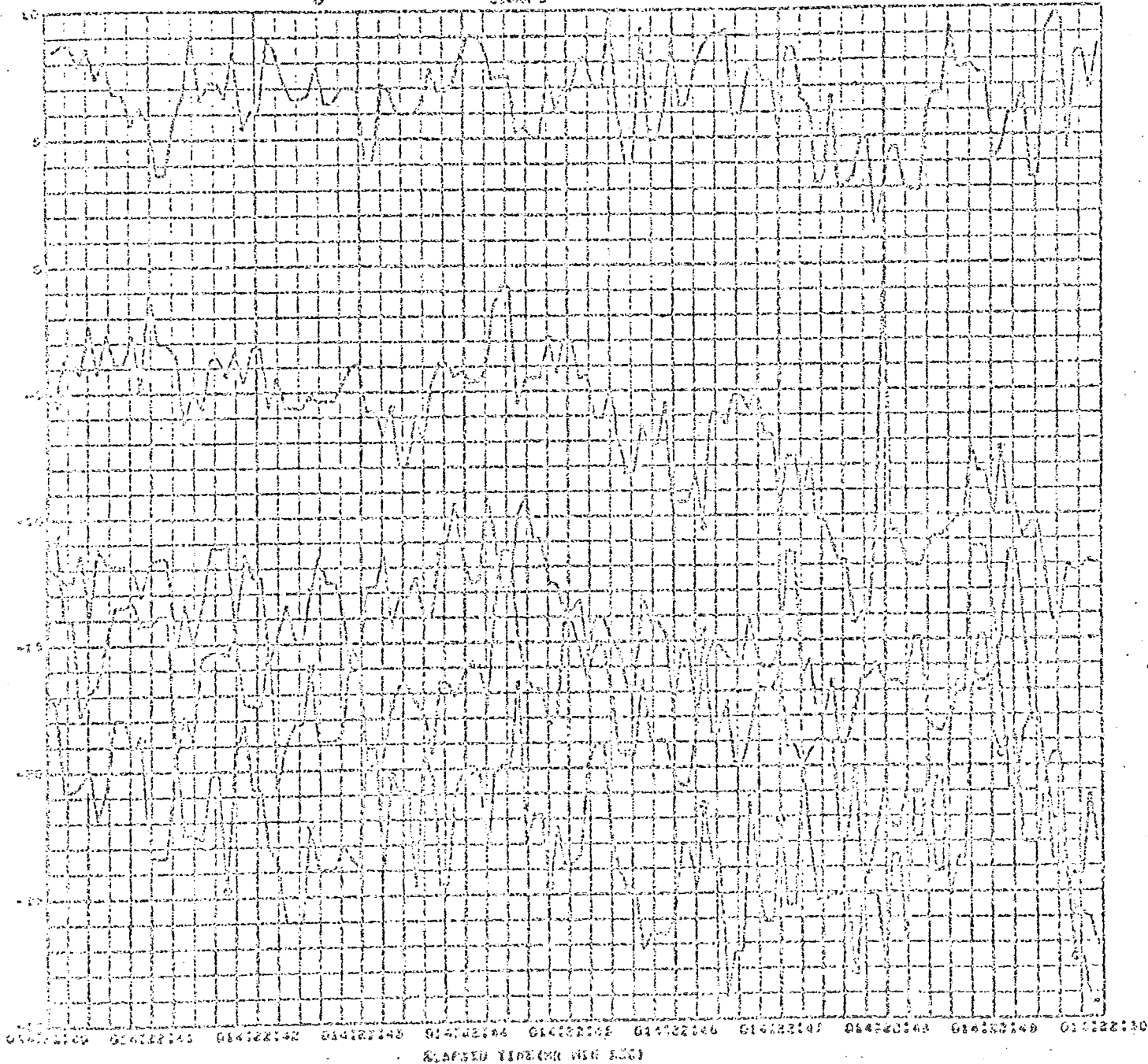


FIGURE 3. TIME HISTORY OF RADAR CROSS-SECTION
($\theta = 2.5, 5, 25, 35, 45^\circ$)

DELOR SIGMA 3 VEL FLY 2 RUM 3 200FT 251 4FT TAPE 20319 02/10/60
 0.120000 91605.620 TO 91700.500 SEC. 02/10/60
 COEFFICIENT OF VARIATION= 0.720057 2.00 PERCENT= 27.4000 5 PERCENT= 24.0000 15 DEGREES OF FREEDOM
 1000000 RANGE= -24.00000 TO 3.70000 RANGE = 0.400000 RANGE = 4.400000 RANGE = -0.800000 RANGE = 4.200000
 COEFFICIENT OF VARIATION= -0.504000

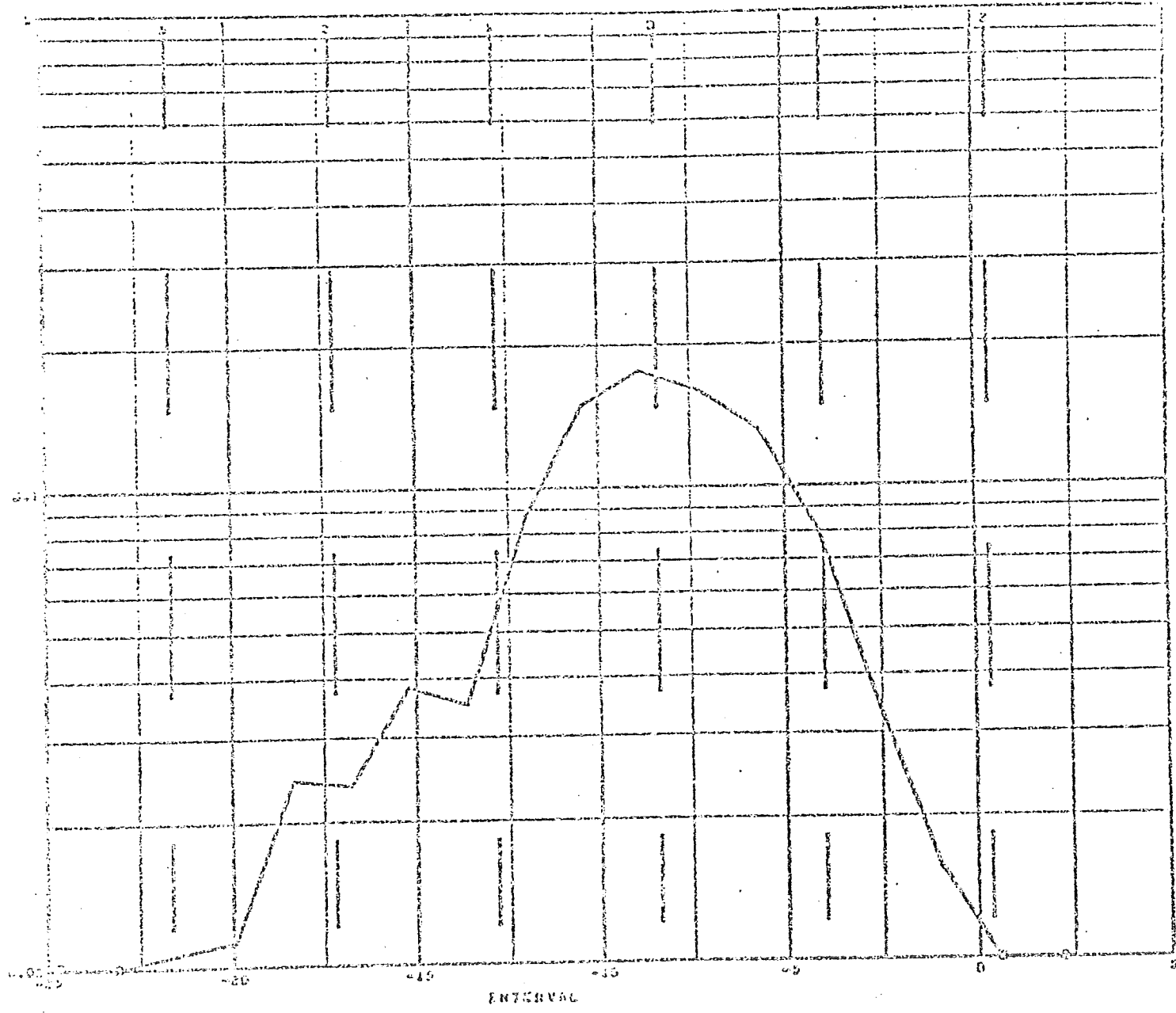


FIGURE 4. PROBABILITY DENSITY FUNCTION OF RADAR CROSS-SECTION

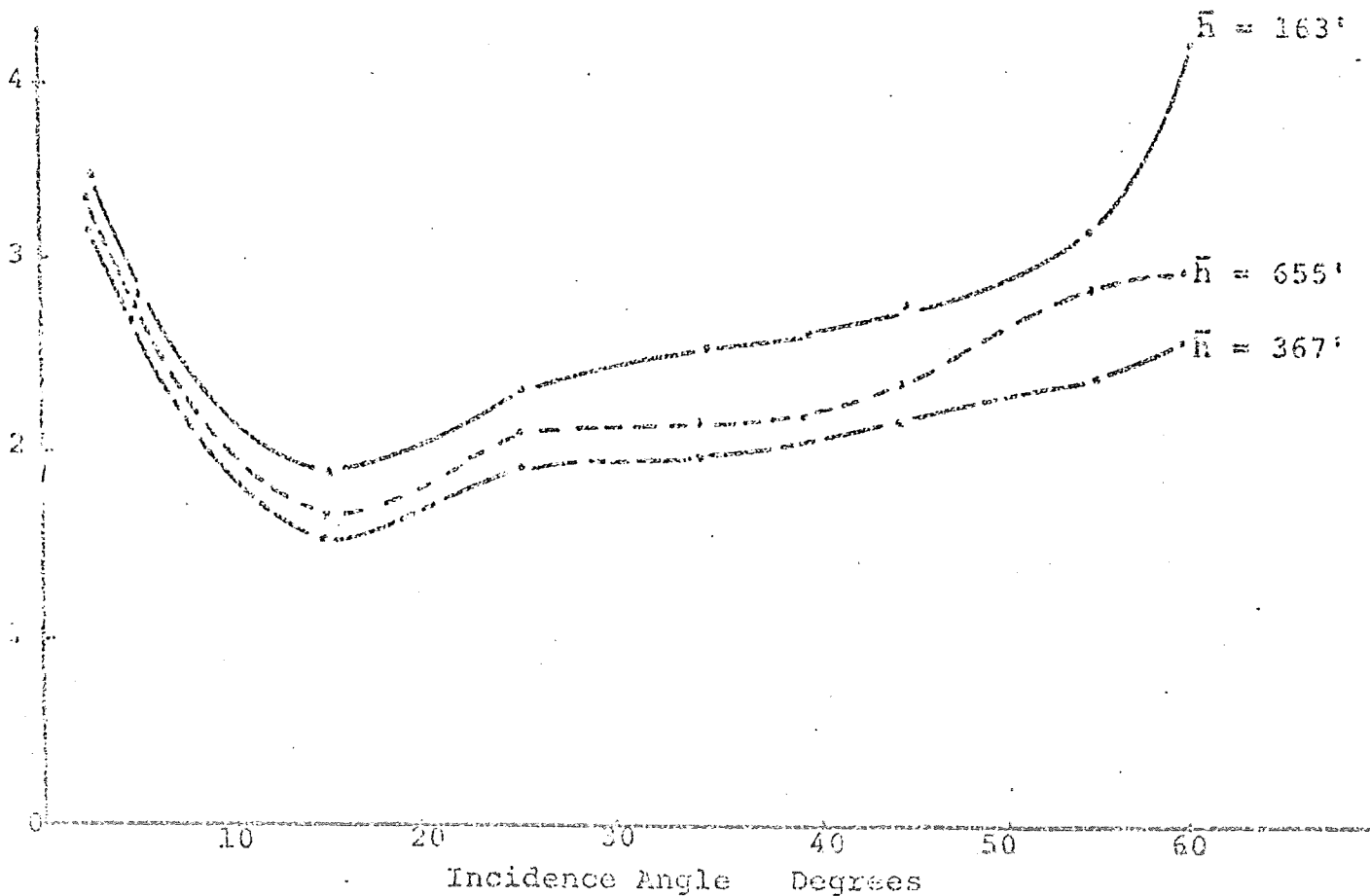
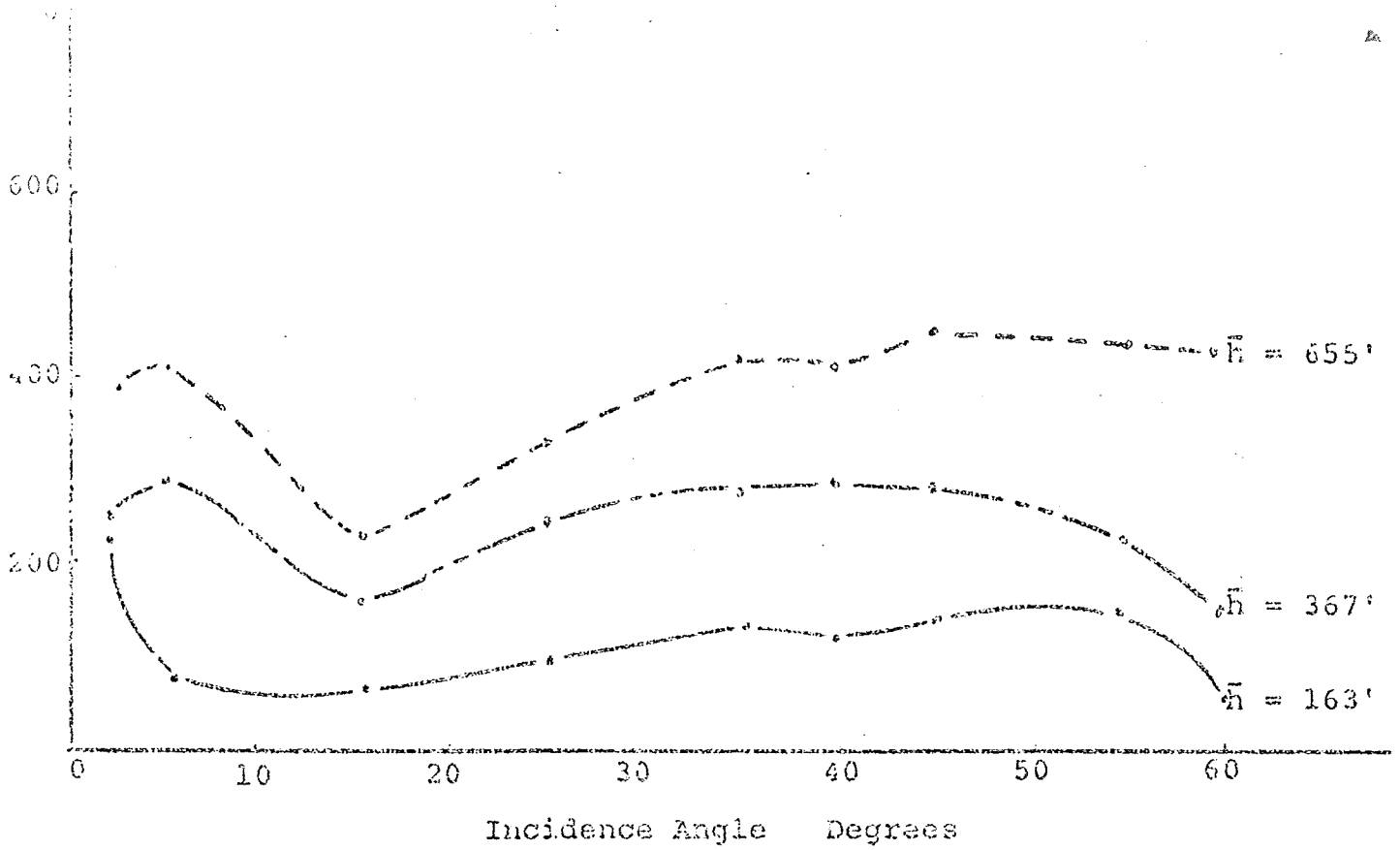


FIGURE 5. VARIANCE AND SURFACE DECORRELATION DISTANCES FOR DESCENDING ALGORITHMS

or

$$\begin{pmatrix} \omega_{d0} \\ \omega_{dH} \\ \omega_{dL} \end{pmatrix} = \frac{4\pi V}{\lambda} \begin{pmatrix} \sin \Theta_0 \\ \sin \Theta_0 \langle \cos \phi \rangle \\ \cos \Theta_0 \langle \sin \phi \rangle \end{pmatrix} \quad (28)$$

with a corresponding power density spectrum prior to the detector (Broderick and Hayre, 1967) of

$$\begin{aligned} W_{AA}(f) = & \frac{E_0^2}{8} e^{-\phi_0^2} \langle R(\omega) \rangle \left(\frac{f_c}{f-f_c} \right)^2 \exp \left[-R_R \left| \frac{f}{f_c} \right| + 2 \left(\frac{f-f_0 \sin \Theta_0}{B} \right)^2 \right] \\ & + \frac{\mu_u^2 E_0^2}{8} \langle R(\omega) \rangle \left(\frac{f_c}{f-f_c} \right)^2 \exp \left[-R_R \left| \frac{f}{f_c} \right| + \left(\frac{f-f_0 \sin \Theta_0}{B_u} \right)^2 \right] \\ & + \frac{\mu_L^2 E_0^2}{8} \langle R(\omega) \rangle \left(\frac{f_c}{f-f_c} \right)^2 \exp \left[-R_R \left| \frac{f}{f_c} \right| + \left(\frac{f-f_0 \cos \Theta_0}{B_L} \right)^2 \right] \end{aligned} \quad (29)$$

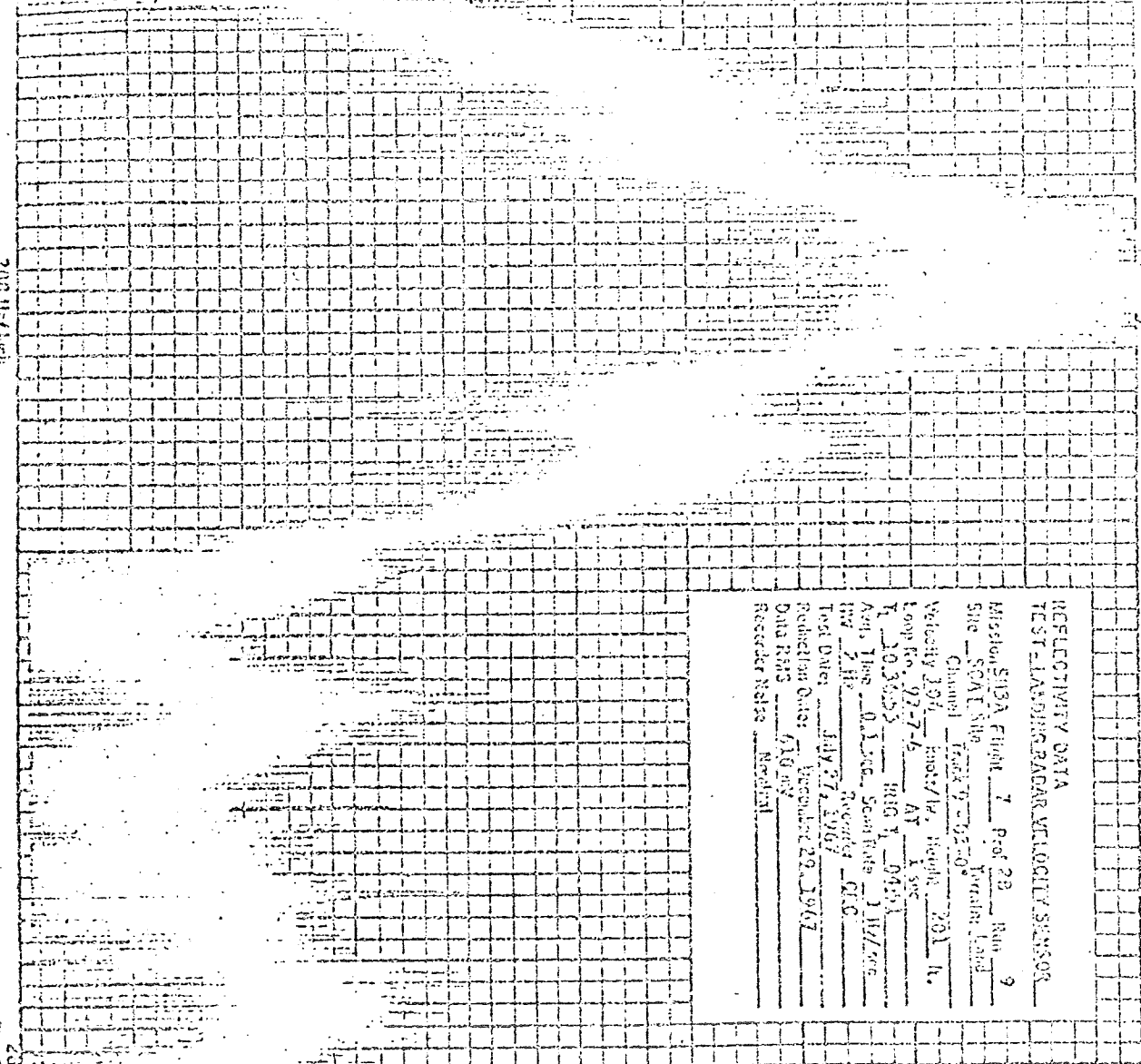
where the doppler shifted carrier $f_c = (2v/c) f_0$, B is the bandwidth for the smooth surface component ($f_0 \bar{\epsilon}$) and B_u (Hayre, and Broderick, 1967) is the bandwidth due to the amplitude modulation caused by the surface variance or for $V_T \ll c$,

$$B_u \sim V_T / \bar{\epsilon}$$

The relative magnitude of a variance component μ_u^2 can be seen in Figure 6 where the basic frequency occurs at 290 cps and multiple harmonics due to the detector.

FIGURE 6. NON-GAUSSIAN DOPPLER SPECTRA

200 Hz/line



REFLECTIVITY DATA
TEST-LANDING RADAR VELOCITY SENSOR

Mission SUDA Flight 7 Prof 28 Run 9
Site SVALBARD Track 9 02:30* Terrain Level
Channel _____ Alt _____ Height 201 ft.
Velocity 204 knots/hr, Height 201 ft.
Loop No. 92-7-6 AT 1 sec
T 20.3625 H000 1 0453
Avg. Time 0.1 sec Scan Rate 1 1/2 sec
TWR 2 Hz Records CLC
Test Dates July 27, 1967
Reduction Date December 29, 1967
Data RMS 610 ms
Recorder Name Mardell

2000

July 69

CONCLUSION

In the analysis of pulse radar systems the average clutter power is defined as

$$P_{cl} = \frac{1}{2\sigma} \int_{-\infty}^{\infty} \int_{-\infty}^{\infty} \gamma \sin \theta_0 |u(t-\tau)|^2 d\omega dR \quad (30)$$

where σ represents the target cross-section, θ_0 the depression angle, $d\omega$ the radial width, dR the ground width, $u(t-\tau)$ the return signal, and γ the backscattering coefficient (mean) for typical ground or sea clutter.

Similarly for a cw radar system, it has been assumed that the power density spectrum has the form

$$W_{cl}(f) = \frac{E_s^2}{8} R(\omega) \left(\frac{f_c}{f-f_c} \right)^2 \exp \left[-R_R \left| \frac{f}{R} \right| + z \left(\frac{f-f_c}{R} \right)^2 \right] \quad (31)$$

where the slope of the mean curve R_R is used to predict a terrain bias error. As shown in Eq. (29) fluctuation errors are produced by the surface variance terms (M_L^2, M_H^2) and under certain conditions of velocity and altitude the doppler spectrum becomes non-Gaussian producing more significant errors than the terrain bias error.

It appears then that in the analysis of either a pulse or cw system that the mean back-scattering curve can be used with confidence only if the variance terms are adequately smoothed for the particular altitude or velocity. Due to the predominant effect of the variance terms at low altitudes and velocities,

future published curves of radar back-scattering cross-section should include the variance as well as the mean value.

REFERENCES

- Beckmann, P. and A. Spizzichino. The Scattering of Electromagnetic Waves from Rough Surfaces, New York: MacMillan Company, 1963, pp. 119-151.
- Broderick, R. F. "New Radar Systems Will Map the Planets," Electronics, Vol. 40, No. 2 (January, 1967), pp. 119-120.
- Broderick, R. F. and H. S. Hayre. Doppler Return from a Random Rough Surface, University of Houston, Wave Propagation Laboratories, Department of Electrical Engineering, Tech. Rept. TR-68-7, May, 1968.
- Hayre, H. S. and R. F. Broderick. Modulation of an Incident Waveform by a Random Rough Surface, University of Houston, Wave Propagation Laboratories, Department of Electrical Engineering, Tech. Rept. TR-68-3, April, 1968.